

Document downloaded from:

<http://hdl.handle.net/10251/94086>

This paper must be cited as:

Pastor Navarro, C.; Sánchez González, L.; Chiralt A.; Cháfer Nácher, MT.; González Martínez, MC. (2013). Physical and antioxidant properties of chitosan and methylcellulose based films containing resveratrol. *Food Hydrocolloids*. 30(1):272-280.  
doi:10.1016/j.foodhyd.2012.05.026



The final publication is available at

<http://doi.org/10.1016/j.foodhyd.2012.05.026>

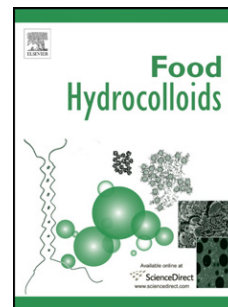
Copyright Elsevier

Additional Information

# Accepted Manuscript

Physical and antioxidant properties of chitosan and methylcellulose based films containing resveratrol

Clara Pastor, Laura Sánchez-González, Amparo Chiralt, Maite Cháfer, Chelo González-Martínez



PII: S0268-005X(12)00136-1

DOI: [10.1016/j.foodhyd.2012.05.026](https://doi.org/10.1016/j.foodhyd.2012.05.026)

Reference: FOOHYD 2017

To appear in: *Food Hydrocolloids*

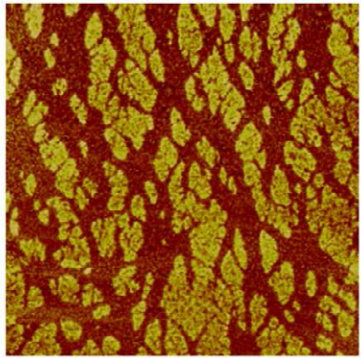
Received Date: 15 February 2012

Revised Date: 24 May 2012

Accepted Date: 29 May 2012

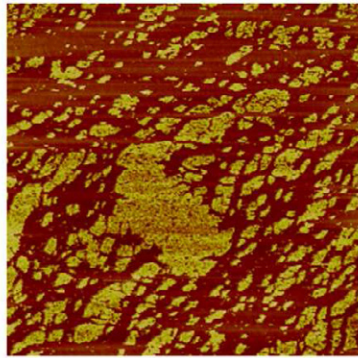
Please cite this article as: Pastor, C., Sánchez-González, L., Chiralt, A., Cháfer, M., González-Martínez, C., Physical and antioxidant properties of chitosan and methylcellulose based films containing resveratrol, *Food Hydrocolloids* (2012), doi: 10.1016/j.foodhyd.2012.05.026.

This is a PDF file of an unedited manuscript that has been accepted for publication. As a service to our customers we are providing this early version of the manuscript. The manuscript will undergo copyediting, typesetting, and review of the resulting proof before it is published in its final form. Please note that during the production process errors may be discovered which could affect the content, and all legal disclaimers that apply to the journal pertain.



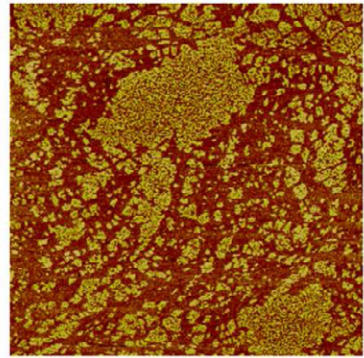
0.0 5.0  $\mu\text{m}$

**CH**



0.0 5.0  $\mu\text{m}$

**CH-R10**



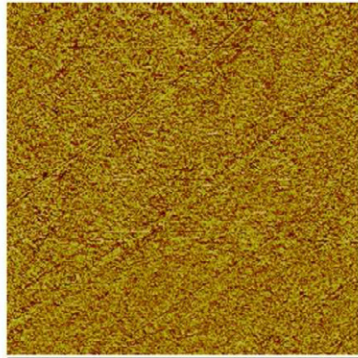
0.0 5.0  $\mu\text{m}$

**CH-R100**



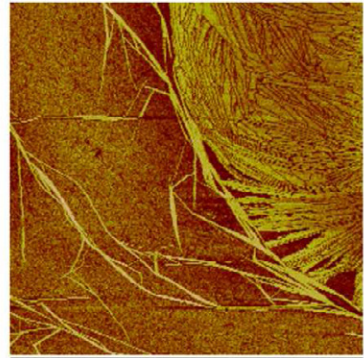
0.0 5.0  $\mu\text{m}$

**MC**



0.0 5.0  $\mu\text{m}$

**MC-R10**



0.0 5.0  $\mu\text{m}$

**MC-R100**

**Physical and antioxidant properties of chitosan and methylcellulose based films  
containing resveratrol**

Clara Pastor, Laura Sánchez-González, Amparo Chiralt, Maite Cháfer and Chelo

González-Martínez\*

Departamento de Tecnología de Alimentos – Instituto de Ingeniería de Alimentos para el Desarrollo.

Universitat Politècnica de València, Valencia, Spain.

(\* *Telephone*: 0034 96 387 70 00 *Ext.* 73656 *Fax*: 0034 96 387 73 69 *e-mail*: [cgonza@tal.upv.es](mailto:cgonza@tal.upv.es)

---

**Abstract**

New trends in edible films focus on the improvement of their functionality through the incorporation of active compounds, such as antimicrobial or antioxidant agents. Resveratrol is a natural antioxidant found in a variety of plant species, such as grapes, and could be used for minimizing or preventing lipid oxidation in food products, retarding the formation of oxidation products, maintaining nutritional quality and prolonging the food shelf life. The aim of this work was to develop and characterize two different polymeric composite films (made with chitosan (CH) and methylcellulose (MC)) containing different amounts of resveratrol. This compound could be incorporated efficiently into both films, but provoke structural changes in the matrices, which became less stretchable (65-70% reduction of deformation at break at the greatest resveratrol content) and resistant to fracture (26 and 54% reduction of tensile at break for MC and CH, respectively, at the greatest resveratrol content) more opaque (significant reduction of the internal transmittance) and less glossy (about 60-65% reduction of gloss at the greatest resveratrol content). Film barrier properties were hardly improved by the presence of resveratrol; water vapour and oxygen permeability tend to slightly decrease when resveratrol was incorporated into both polymers.

26 Composite films showed antioxidant activity, which was proportional to the resveratrol  
concentration in the film. None of the films showed antimicrobial activity against  
28 *Penicillium italicum* and *Botrytis cinerea*. Thus, these films could be applied to food  
products which are sensitive to oxidative processes to prolong their shelf life.

30

*Keywords: microstructure, water vapour permeability, oxygen permeability,  
32 mechanical and optical properties, antioxidant activity*

### 34 **1. Introduction**

Bioactive edible films may be considered as a natural and biodegradable alternative to  
36 chemical preservatives in order to extend food shelf life. Besides acting as protective  
barriers, these films can be used as carriers of bioactive compounds, such as  
38 antimicrobials and antioxidants. Among the biopolymers used to formulate edible films,  
cellulose derivatives such as methylcellulose (MC), are interesting film forming  
40 compounds, as they are odourless, tasteless and biodegradable (Krochta and Mulder-  
Johnston, 1997). Another biopolymer with excellent film forming ability is chitosan (Li  
42 et al. 1992). This non-toxic compound, obtained by deacetylation of chitin, a structural  
component present in the shell of some crustaceans, presents antimicrobial properties.  
44 Edible films should be designed to fulfil a number of requirements, such as having  
proper mechanical properties, good appearance (adequate gloss and transparency) and  
46 water and gas barrier properties.

Resveratrol (3,5,4'-trihydroxystilbene) is a natural polyphenol found in a variety of  
48 plant species such as grapes, mulberries and peanuts. This molecule possesses  
interesting antioxidant and antifungal properties. Antioxidant capacity of resveratrol has  
50 largely been studied in vitro by applying physico-chemical methods. Murcia and

Martínez-Tomé (2001) characterized the antioxidant activity of this stilbene and compared it with those obtained for other antioxidants (alpha-tocopherol, vanillin, butylated hydroxytoluene (BHT), butylated hydroxyacetone (BHA), phenol, propyl gallate, sodium tripolyphosphate). Among the tested molecules, only BHA showed a greater antioxidant activity than resveratrol to inhibit lipid peroxidation. Soto-Valdez et al. (2010) reported that resveratrol had a higher radical-scavenging capacity than propyl gallate, ascorbic acid, and  $\alpha$ -tocopherol. Gulçin (2010) demonstrated that 30  $\mu\text{g/mL}$  of resveratrol inhibited 89.1% of the lipid peroxidation of a linoleic acid emulsion.

As regards the antifungal activity, Hoos and Blaich (1990) and Adrain et al. (1997) described inhibitory effects of resveratrol on *B. cinerea* conidia in solid and liquid culture medium. Filip et al. (2003) reported the effectiveness of resveratrol against filamentous fungi *Penicillium expansum* and *Aspergillus niger* and yeast. *A.niger* remains the most sensitive strain out of the three tested genera.

Little information about the incorporation of resveratrol into films is available at the moment. Only some works on resveratrol incorporation into polylactic acid (PLA) based films, obtained by a blow-extrusion process, have been found (Soto-Valdez et al. 2011). The effect of resveratrol on PLA film properties was studied, and the kinetics of the diffusion of resveratrol from the PLA matrix into ethanol was analysed. These authors recommended these films be used as antioxidant release membranes for a variety of pharmaceutical, medical, and food applications.

The aim of this work was to characterize films based on different polysaccharides (chitosan or methylcellulose) containing resveratrol in different polymer:resveratrol ratios (1:0.01 and 1:0.1) by analysing their microstructure, water vapour and oxygen barrier, mechanical and optical properties and to study the effect of resveratrol incorporation on their antioxidant and antifungal properties.

76

## 2. Materials and methods

### 78 2.1. Raw materials

Food Grade Methylcellulose (MC, CAS number 9004-67-5), medium molecular weight  
80 chitosan (CH, CAS number 9012-76-4) with a deacetylation degree of 75-85% and  
resveratrol (R, CAS number 501-36-0), supplied by Sigma-Aldrich Química (Madrid,  
82 Spain), were used to prepare the film-forming dispersions.

### 84 2.2. Preparation of film forming dispersions

To obtain film-forming dispersions (FFDs), 2% (wt) methylcellulose was dispersed in  
86 distilled water. Chitosan (1% wt) was dispersed in an aqueous solution of glacial acetic  
acid (0.25% v/v) and stirred overnight at room temperature. The corresponding amount  
88 of resveratrol (R) was dissolved in 96% ethanol and added to the polymer solutions to  
reach a polymer:ethanol:resveratrol ratio of 1:1:0.01 and 1:1:0.1 in the FFDs.  
90 Afterwards, these were homogenized in a rotor-stator ultraturrax DI25 at 13.500 rpm for  
4 min. Resveratrol based FFDs were properly protected from light using amber glass  
92 flasks during handling.

Pure methylcellulose and chitosan FFDs (resveratrol free) were characterized as  
94 controls. In these cases, the same ratio of ethanol as in the films containing R was  
incorporated into the FFD to ensure the polymer had the same aqueous media solvent  
96 properties in all cases.

The mixtures were degasified for 10 min at room temperature by means of a vacuum  
98 pump (Diaphragm vacuum pump, Wertheim, Germany).

### 100 2.3. Film preparation

Films were obtained by casting. FFDs were poured onto a framed and levelled  
102 polytetrafluorethylene (PTFE) plate ( $\phi = 15$  cm) and were dried for 48 h, under natural  
convection, at 25°C and 60% relative humidity (RH). Film thickness was controlled by  
104 pouring onto the PTFE plate the amount of FFD that will provide a surface density of  
solids in the dry films of 56 g/m<sup>2</sup> in all formulations. The drying process was carried out  
106 in darkness to protect the FFDs from the light. Dry films were peeled off the casting  
surface and preconditioned prior to testing in desiccators at 25°C and 75% RH (by using  
108 an oversaturated NaCl solution). A digital micrometer (Electronic Digital Micrometer,  
Comecta S.A., Barcelona, Spain) was used to measure the film thickness in at least five  
110 random positions around the film.

## 112 *2.4. Film characterization*

### 114 *2.4.1. Scanning electron microscopy (SEM)*

114 Microstructural analysis of the films was carried out by SEM using a scanning electron  
microscope (JSM-6300, JEOL Ltd., Tokyo, Japan). Film samples were maintained in a  
116 desiccator with P<sub>2</sub>O<sub>5</sub> for two weeks to ensure that no water was present in the sample.  
Then, films were frozen in liquid N<sub>2</sub> and cryofractured to observe the cross-section of  
118 the samples. Films were fixed on copper stubs, gold coated, and observed using an  
accelerating voltage of 15 kV.

120

### 122 *2.4.2. Atomic force microscopy (AFM)*

122 The surface morphology of dried film samples (equilibrated in a desiccator with P<sub>2</sub>O<sub>5</sub>)  
was analysed using an atomic force microscope (Multimode 8, Bruker AXS, Santa  
124 Barbara, USA) with a NanoScope® V controller electronics. The resulting data were  
transformed into a 3D image. Measurements were taken from several areas of the film



126 surface (50x50 and 5x5  $\mu\text{m}$ ) using the tapping mode. According to method ASME  
128 B46.1 (ASME, 1995), the following statistical parameters related with sample  
130 roughness were calculated: average roughness (Ra: average of the absolute value of the  
132 height deviations from a mean surface), root-mean-square roughness (Rq: root-mean-  
134 square average of height deviations taken from the mean data plane). Phase Imaging  
mode derived from Tapping Mode, that goes beyond topographical data to detect  
variations in composition, adhesion, friction, viscoelasticity, and other properties,  
including electric and magnetic, was also applied. Three replicates were considered to  
obtain these parameters.

#### 136 2.4.3. Film thickness

A hand-held digital micrometer (Electronic Digital Micrometer, Comecta S.A.,  
138 Barcelona, Spain) was used to measure film thickness in six different points of the same  
film.

140

#### 2.4.4. Moisture content

142 Film samples were dried in triplicate at 60°C for 24 h in a natural convection oven and  
for 24 h more in a vacuum oven in order to determine their moisture content.

144

#### 2.4.5. Water vapour permeability

146 The water vapour permeability (WVP) of films is commonly measured by using a  
modification of the ASTM E96-95 (ASTM, 1995) gravimetric method using Payne  
148 permeability cups (Elcometer SPRL, Hermelle/s Argenteau, Belgium) of 3.5 cm  
diameter. For each type of film, measurements were replicated seven times and WVP  
150 was calculated following the methodology described by Gennadios et al. (1994), at 25°C

and a 75-100% relative humidity gradient, which was generated by using an  
152 oversaturated NaCl solution and pure water, respectively. To determine WVP, the cups  
were weighed periodically (each 2 h, for 10 h) after the steady state was reached using  
154 an analytical balance ( $\pm 0.0001$  g). Then the slope obtained from the regression analysis  
(5 points) of weight loss data as a function of time was used to calculate WVP,  
156 according to ATSM (1995).

#### 158 2.4.6. Oxygen permeability

The oxygen permeability of the films (OP) was measured in triplicate by using an  
160 oxygen permeation measurement system (OX-TRAN 1/50, Mocon, Minneapolis, USA)  
at 25°C and 75% RH (ASTM, 2005). A sample of the film (50 cm<sup>2</sup>) was placed in a test  
162 cell and pneumatically clamped in place. Films were exposed to pure nitrogen flow on  
one side and pure oxygen flow on the other side. An oxygen sensor read permeation  
164 through the barrier material and the rate of permeation or oxygen transmission rate was  
calculated taking into account the amount of oxygen and the area of the sample. Oxygen  
166 permeability was calculated by dividing the oxygen transmission rate by the difference  
in oxygen partial pressure between the two sides of the film, and multiplying by the  
168 average film thickness.

#### 170 2.4.7. Mechanical properties

A texture analyser (TA-XTplus, Stable Micro Systems, Surrey, United Kingdom) was  
172 used to measure the mechanical properties of films equilibrated at 75% HR and 25°C.  
Strips of films (25.4 mm wide and 100 mm long) were mounted in the tensile grips  
174 (A/TG model) and stretched at a rate of 50 mm/min until breaking. The elastic modulus  
(EM) and tensile strength (TS) and percentage of elongation (%E) at break were

176 determined from stress-strain curves, obtained from force-deformation data. The  
experiments were carried out at 25°C on twelve replicates from each film.

178

#### 2.4.8. Optical properties

180 The optical measurements were taken in films previously equilibrated at 25°C and 75%  
RH. CIE-L\*a\*b\* coordinates chroma ( $C^*_{ab}$ ) and hue ( $h^*_{ab}$ ) of the films were obtained  
182 through the surface reflectance spectra determined by means of a spectrophotometer  
(CM-3600d, Minolta Co., Tokyo, Japan) with a 10 mm diameter window, using D65  
184 illuminant/10° observer. Measurements were taken on black and white backgrounds and  
the reflectance infinite ( $R_{\infty}$ ) was determined.

186 The whiteness index (WI) was calculated by applying equation 1:

$$WI = 100 - \sqrt{(100 - L^*)^2 + a^{*2} + b^{*2}} \quad \text{Eq. (1)}$$

188

The internal transmittance ( $T_i$ ) of the films was determined by applying the Kubelka–  
190 Munk theory (Hutchings, 1999) for multiple scattering to the reflection spectra,  
following the methodology described by Pastor et al. (2010).

192 The gloss of the films was measured at a 60° incidence angle according to the ASTM  
standard D-523 (ASTM, 1999), using a flat surface gloss meter (Multi-Gloss 268,  
194 Minolta Co., Tokyo, Japan). All results are expressed as gloss units (GU), relative to a  
highly polished surface of black glass standard with a value near to 100.

196 All measurements were taken in quintuplicate for each film at room temperature.

#### 2.4.9. Antioxidant activity

The potential antioxidant power of films was measured via the in vitro determination of  
200 the free radical scavenging effect on 2,2-Diphenyl-1-picrylhydrazyl (DPPH·) radical,

following the methodology described by Brand-Willians et al. (1995). This method is  
 202 based on the reduction of DPPH· in an alcoholic solution in the presence of a hydrogen-  
 donating antioxidant, due to the formation of the non-radical form of DPPH in the  
 204 reaction. In the radical form, this molecule shows absorbance at 517 nm, which  
 disappears after accepting an electron or hydrogen radical from an antioxidant  
 206 compound thus becoming a stable diamagnetic molecule (Matthäus, 2002).

To this end, dry films (0.12 and 0.012 g, respectively for the film with a lower and  
 208 higher concentration of resveratrol) were previously dissolved in 15 (for CH films) or 5  
 (for MC) mL deionised water and maintained under magnetic stirring for 12 h at 25°C.

210 In all cases 0.5 mL of the different appropriately diluted samples were added to 3.5 mL  
 of methanol solution of DPPH· (0.030 g l<sup>-1</sup>).

212 The decrease in absorbance at 25°C was determined by using a spectrophotometer  
 (Helios Zeta UV-Vis, Thermo Fisher Scientific, United Kingdom) at 515 nm.

214 Measurements were taken every 15 min until the reaction reached a plateau. The DPPH·  
 concentration (mM) in the reaction medium was calculated from the calibration curve

216 (Eq. 2) determined by linear regression ( $R^2 = 0.999$ ):

$$A_{515\text{nm}} = 11.36x[\text{DPPH}\cdot] - 0.037 \quad \text{Eq. (2)}$$

218

The percentage of remaining DPPH· (%DPPH<sub>REM</sub>) was calculated according to  
 220 equation 3:

$$\%DPPH_{\text{REM}} = \frac{[\text{DPPH}\cdot]_{\text{T}}}{[\text{DPPH}\cdot]_{\text{T}=0}} \quad \text{Eq. (3)}$$

222 where,

(DPPH)<sub>T</sub> is the concentration of DPPH· at the steady state.

224 (DPPH)<sub>T=0</sub> is the concentration of DPPH· at the initial reaction time.

226 The percentage of remaining DPPH· was plotted *versus* the molar ratio of antioxidant to  
DPPH· (moles of resveratrol/mol DPPH·) to obtain the amount of antioxidant necessary  
228 to decrease the initial DPPH· concentration by 50% (EC<sub>50</sub>). This parameter was used to  
measure the antiradical activity of the films. EC<sub>50</sub> values were expressed in terms of  
230 moles of resveratrol per mole of DPPH· and also in terms of kg film per mole DPPH·.  
The antioxidant activity of 8.98 M resveratrol ethanol solution was also determined,  
232 using the same methodology.

#### 234 2.4.10. Microbiological analysis

To determine the possible antimicrobial activity of the films, *P. italicum* (CECT 2294)  
236 and *B. cinerea* (CECT 2100) (CECT 2574) supplied by Colección Española de Cultivos  
Tipos (CECT, Burjassot, Spain) were used. Both were kept frozen (-25°C) in Potato  
238 Dextrose Broth (PDB) (Scharlab, Barcelona, Spain) supplemented with 30% glycerol  
(Panreac, Barcelona, Spain). The fungi were inoculated on Potato Dextrose Agar (PDA)  
240 and incubated at 25°C until sporulation. Then the cells were re-suspended in  
physiological water with 0.1% Tween 80. The cells were counted in a haemocytometer  
242 and diluted to a concentration of 10<sup>5</sup> spores per mL. Aliquots of PDA (20 g) were  
poured into Petri dishes. After the culture medium solidified, the diluted spore solution  
244 was inoculated on the plate surface and films of the same diameter as the Petri dishes  
were placed on the inoculated surface (adapted from Kristo et al. 2008). Inoculated and  
246 uncoated PDA Petri dishes were used as control. Plates were then covered with parafilm  
to avoid dehydration and stored at 20°C for 5 days. All tests were run in duplicate.

248

#### 2.5. Statistical analysis

250 A statistical analysis of data was performed through a one-way analysis of variance  
using Statgraphics® Plus for Windows 5.1. Homogeneous sample groups were obtained  
252 by using LSD test (95% significance level).

### 254 **3. Results and discussion**

#### *3.1. Film microstructure*

256 Figure 1 shows the SEM micrographs of the cross section of the obtained films with CH  
or MC with and different amounts of resveratrol. Pure CH film showed a smooth  
258 appearance in agreement with an ordered packaging of polymer chains whereas when it  
contains resveratrol a coarse aspect can be appreciated, more accused when the  
260 resveratrol concentration increases. This suggests that the presence of stilbene difficult  
the chain entanglements giving rise to more disordered network. In the case of MC,  
262 SEM micrographs does not reveal appreciable irregularities in the polymer matrix when  
resveratrol was incorporated at any concentration, but an increase in the film thickness  
264 was promoted, the greater the resveratrol concentration, the thickest the film. This was  
also observed for the CH films as can be seen en Table 1, where the values of the  
266 different film thicknesses are shown. These features reveal that resveratrol molecules  
affect the chain rearrangement in the films for both, MC and CH, modifying the film  
268 microstructure. The changes are more intense for CH films where the enhancement of  
film thickness is near 30% (only 14% for MC) and the cross section of the film shows  
270 more pronounced irregularities.

Figure 2 shows the AFM images of the surface of the films where the changes in the  
272 surface topography induced by resveratrol incorporation can be seen. These are  
especially relevant when the highest concentration was used, where a notable increase  
274 in the surface roughness can be appreciated for the CH films. For MC films, a different

surface aspect due to the resveratrol incorporation can be observed, but statistical  
276 roughness parameters (Ra, Rq) did not reveals an actual increase in roughness.

A Phase Imaging analysis was also obtained from the Tapping Mode AFM data, which  
278 allows us to detect variations in composition, adhesion, friction, viscoelasticity and  
other properties in the material surface, providing material property contrast. Figure 3  
280 shows the phase images of the obtained films, where very clear differences can be  
observed between samples at the nano-scale level. Surface of CH films shows two  
282 different phases which could correspond to a more crystalline (less hydrated, harder)  
zones, dispersed in an amorphous (more hydrated, softer) zone. Zhang et al. (2006)  
284 described the development of crystallinity in CH matrices due to the formation of  
hydrogen bonds between flexible chains showing a characteristic X-ray diffraction  
286 pattern with two pecks; the strongest one at  $2\theta$  of about  $20^\circ$  and a weak peak at  $10^\circ$   
(crystal forms II and I, respectively). The more dominate polymorph corresponds to  
288 hydrated crystals where water molecules are incorporated in to the crystal lattice which  
is normally detected by a broad crystalline peak in the corresponding X-ray pattern  
290 (Wan et al. 2006). It is remarkable that the presence of resveratrol modify the size and  
distribution of the “crystalline” zones, as much as its concentration increases in the film.  
292 Isolated, wider “crystalline” zones together with other very small can be observed.  
Polidispersity of the crystalline zone size distribution increases when resveratrol  
294 concentration increases. This can be attributed to the fact the resveratrol molecules  
(more or less heterogeneously distributed) between the CH chains modify the possibility  
296 of the hydrogen bond formation between chains, limiting the growth of crystalline zones  
where the stilbene molecules are more present by creating steric hindrances for chain  
298 bonding.

In the case of MC a more homogenous surface can be observed from the phase analysis.

300 Different authors (Donhowe and Fennema, 1993a and b) describe extensive association  
of MC by hydrogen bonding and hydrophobic association which induces crystallization  
302 likely reinforces the film matrix. The very homogeneous, ordered structure, which is  
revealed by phase image of MC films, is coherent with the formation of chain  
304 association in crystalline lattices. Nevertheless, in samples with the highest  
concentration of resveratrol, crystal of this compound could be observed, showing the  
306 typical dendritic shapes of crystal growth of pure molecular compounds. This could not  
be observed for MC samples with the lowest resveratrol content, but was present in all  
308 the observations with the highest content. This means that resveratrol separates in the  
MC film forming dispersion during the film drying step when its saturation level is  
310 reached, in the form of crystals, as described by Caruso et al. (2004). The resveratrol  
concentration used in the FFD is well above its critical micelle concentration (CMC  
312 around 12.5-37  $\mu\text{M}$ , depending on pH), thus leading to a non-molecularly dispersed  
compound which forms molecular aggregates. These could be crystals with a planar  
314 structure which establishes a network through hydrogen bonds, (Caruso et al. 2004).  
This phenomenon was not observed for CH films probably due to the highest viscosity  
316 of CH in the film forming dispersions (Sánchez-González et al. 2001a) which inhibit the  
resveratrol crystal growth when it reach the saturation level during the film drying step.

318 At the lowest concentration, probably the resveratrol saturation level was reached when  
the MC solution has enough viscosity to inhibit crystal formation and it remains more or  
320 less homogeneously distributed in the matrix, at molecular level, between the MC chains.  
The presence of resveratrol can cause a large increase in the d101 spacing of the crystal  
322 lattice as occurs when plasticizers with low molecular weights are incorporated in the  
MC films (Donhowe and Fennema, 1993a). This will affect the films thickness,



324 increasing its value as can be seen in Table 1: the greater the amount of resveratrol in  
the film, the thicker the film.

326

### 3.2. *Barrier properties*

328 Table 1 shows the mean values and standard deviation of WVP and OP of all films  
equilibrated at 25°C and 75% RH, together with the values of the film moisture content.

330 The WVP values of resveratrol-free films were in the range of those reported by  
Sánchez-González et al. (2011a) and Vargas et al. (2011b) for chitosan and  
332 methylcellulose, respectively. Furthermore, the OP values of pure MC films agree with  
that reported by Donhowe and Fenema (1993a).

334 Significant differences in water vapour and oxygen barrier properties were found due to  
both the nature of the polysaccharide and the concentration of resveratrol in the films.

336 Due to the more hydrophilic nature of chitosan and the presence of greater amount of  
water molecules in the matrix (reflected in the higher values of the equilibrium moisture  
338 content), pure chitosan based films showed higher water vapour permeability and lower  
oxygen permeability than pure methylcellulose, in agreement with previously reported  
340 values (Vargas et al. 2011b) and with others works (Miller and Krochta, 1997). The  
chemical affinity of permeant and film greatly affect permeability values. In this sense,  
342 the low water solubility of oxygen could be responsible for the low OP values in the  
more hydrated CH matrix.

344 The incorporation of resveratrol tended to reduce the water vapour permeability of both  
kinds of films. The lipophilic nature of this stilbene (López-Nicolás and García-  
346 Carmona, 2010) explains the observed effect on the vapour water barrier properties,  
which were only slightly enhanced, in all likelihood due to the low concentration of the  
348 active compound incorporated in the film. This effect was only significant when using

350 methylcellulose, with very small induced differences. It seems to indicate that the structural changes provoked by the resveratrol addition did not imply notable changes for mass transfer rate of water molecules.

352 Oxygen permeability was also slightly affected by the incorporation of resveratrol, this being only significantly reduced ( $p < 0.05$ ) in CH matrices. Although resveratrol seems 354 to induce the formation of more open MC lattices, as commented on above, this did not significantly affect the oxygen mass transfer rate, contrary to that observed by other 356 authors (Donhowe and Fennema, 1993a) for low molecular weight plasticizers. In CH films, OP decreased significantly ( $p < 0.05$ ), which could be related with the more 358 tortuous pathway for the pass of oxygen molecules through the amorphous zones in the matrix as can be observed in Figure 3 from AFM phase image.

360

### 3.3. Mechanical properties

362 The typical tensile strength *versus* Hencky deformation curves obtained during the mechanical test carried out on the films are shown in Figure 1. As can be deduced from 364 this figure, CH films were mechanically more resistant to fracture (greater TS and EM values) than MC films. The values of chitosan films coincide with those reported by 366 Vargas et al. (2011a) and Sánchez-González et al. (2011a), whereas those of MC films were slightly higher than those reported by Vargas et al. (2011b). The incorporation of 368 resveratrol to the films made them shorter and led to them breaking at a lower deformation degree. The greater the resveratrol concentration in the film, the more 370 brittle the film.

Table 2 shows the mechanical properties of films, in terms of tensile strength (TS) and 372 percentage of elongation at break (E%) and elastic modulus (EM). The mechanical response of the films from both polymers showed similar trends when the resveratrol

374 was incorporated into the matrix, in terms of E% and TS. The addition of resveratrol led  
to a decrease in the tensile strength and deformation at break, in turn leading to films  
376 which were less stretchable and resistant to break. This behavior is typical of composite  
films, where the incorporation of non-miscible compounds provokes structural  
378 discontinuities in the polymer network and a reduction in the overall cohesion forces of  
the matrix (Sánchez-González et al. 2010 and 2011a).

380 The effect of resveratrol incorporation on the elastic modulus (EM) parameter was  
dependent on the polymer matrix: it decreased in chitosan composite films, whereas it  
382 increased in MC composite films. The structural changes induced by resveratrol in the  
polymer matrices are responsible for this behavior. In CH films, the dominate formation  
384 of smaller crystalline zones will imply the reduction of the stress-strain relationships  
and so the elastic modulus of the films, whereas the modification of crystalline  
386 arrangement of MC by stilbene seems to increase the cohesion forces of the lattices  
probably by the action of cooperative forces with the resveratrol molecules. The  
388 resveratrol crystal formation in MC films could also contribute to an increase in the film  
rigidity. The decrease in the film stretchability, and the subsequent reduction of the  
390 tensile stress at break, can be also justified by the structural changes promoted by  
resveratrol. CH matrix with smaller and more heterogeneous crystalline zones will be  
392 less resistant to deformation, breaking at low extension degree, whereas the presence of  
resveratrol crystals in the MC films supposes discontinuities in the matrix which favors  
394 film rupture at lower deformation levels.

#### 396 *3.4. Optical properties*

Film transparency was evaluated through the internal transmittance of the samples: the  
398 greater the transmittance value, the more transparent the film. In Figure 2, the spectral

distribution of transmittance ( $T_i$ ) of films equilibrated at 25°C and 75% RH is shown.

400 As can be observed, pure MC and CH films were highly transparent and, in both cases,  
the incorporation of resveratrol provoked a decrease in the  $T_i$  values, thus increasing the  
402 film's opacity. This effect was more pronounced at the highest resveratrol  
concentration. Composite films turned more opaque due to the loss of homogeneity in  
404 the polymer matrix, which is caused by the presence of structural heterogeneities in the  
films with a different refractive index, which promotes light scattering phenomena. The  
406 presence of smaller crystalline zones in the CH films when resveratrol was incorporated  
will promote light scattering, thus increasing the film opacity. In the case of MC, the  
408 more open crystalline lattices containing resveratrol aggregates will also reduce the  
specular light transmission through the films, increasing their opacity.

410 Table 3 shows the values of the colour coordinates, lightness ( $L^*$ ), hue ( $h^*_{ab}$ ) and  
chrome ( $C^*_{ab}$ ), together with the whiteness index (WI) and the gloss of the different  
412 films. In MC composite films, the luminosity, hue and whiteness index significantly  
decreased when the resveratrol content rose, while color saturation ( $C^*_{ab}$ ) increased.  
414 These effects were barely appreciated in the case of chitosan films probably due to the  
fact that no crystals of resveratrol are formed, but only changes in their semi-crystalline  
416 structure with lower impact in light reflection.

Both composite films became less glossy ( $p < 0.05$ ) when the concentration of resveratrol  
418 increased in the films, this effect being more marked in MC composite films. This can  
be attributed to the presence of resveratrol crystals on the film surface, which  
420 contributes to an increased surface heterogeneity and so, a reduction in the gloss. This  
effect has been previously observed by several authors working on composite films  
422 (Pastor et al. 2010; Sánchez-González et al. 2010). The above described structural

changes induced by the resveratrol in the films are responsible for the observed changes  
424 in optical properties.

### 426 3.5. Antioxidant activity

The antioxidant activity of the films was evaluated by means of the dissolution of the  
428 film in a controlled amount of distilled water. Once dissolved, the method described by  
Brand-Willians et al. (1995) based on the DPPH free radical method was applied. At the  
430 pH of the dispersions (6.5 and 4.5 respectively for MC and CH), resveratrol is in  
protonate form, since the  $\text{pH} < \text{PKa}_1 \sim 8.8$  (López-Nicolás and García-Carmona, 2008).  
432 This protonate form needs to be able to exhibit several biological activities, such as  
antioxidant power. From these experiments, the  $\text{EC}_{50}$  values were obtained from the  
434 plot of the % of remaining DPPH· at the steady state *versus* moles of resveratrol/moles  
DPPH· (Fig. 3). This parameter indicates the amount of antioxidant needed to reduce  
436 the initial DPPH concentration to 50%, once the steady-state of the reaction was  
reached. Thus, the lower the  $\text{EC}_{50}$  values, the greater the antioxidant activity of the  
438 tested sample. Table 4 shows the  $\text{EC}_{50}$  values for pure resveratrol and the different  
films, expressed in terms of moles of resveratrol per DPPH· moles and in kg films per  
440 DPPH· mol, by taking into account the amount of resveratrol in each film sample.  
Resveratrol was found to react slowly with the DPPH· (slow kinetic behavior)  
442 coinciding with that reported by Villaño et al. (2007), taking around 100-120 min to  
reach the steady state.  
444 The  $\text{EC}_{50}$  value found for the pure resveratrol was greater than those found by Villaño et  
al. (2007) and Sánchez-Moreno et al. (1998); around 0.50-0.58 moles resveratrol/mole  
446 DPPH·. The different solvent medium (water:ethanol and methanol, respectively) used  
by these authors could explain the observed differences.

448 The obtained values for  $EC_{50}$ , expressed in terms of moles of resveratrol per mole  
DPPH· reflect that no losses of antioxidant activity occurred for resveratrol in the CH  
450 films, since no significant differences were found either in the  $EC_{50}$  values of pure  
resveratrol or of that encapsulated in the CH films. On the contrary,  $EC_{50}$  values for MC  
452 films were slightly higher, which indicates that some loss of antioxidant activity occurs  
in these films. This could be due to the lower extractability of resveratrol from this  
454 matrix which reduces the compound reaction capacity in the solvent medium, but also  
to some degradation of encapsulated resveratrol due to the higher OP of MC films, as  
456 compared with CH films.

When referring  $EC_{50}$  values in terms of kg film per mole DPPH·, the effect of the  
458 antioxidant concentration in the film is clearly shown and, as can be observed, the  
antiradical efficiency increased in line with the resveratrol content in the film.

460 The main conclusion of this test is that the antioxidant efficiency of resveratrol did not  
notable change during film formation, drying and conditioning, which indicates the  
462 great antioxidant potential of these films encapsulating resveratrol.

### 464 3.6. Microbiological analysis

Microbial analysis showed that none of the composite films show antifungal activity  
466 against either *P. italicum* or *B. cinerea*. Filip et al. (2003) found that resveratrol  
presented antifungal activity against *P. expansum* but no information has been found  
468 about *P. italicum*. Regarding *B. cinerea*, the resveratrol concentrations used were higher  
than the minimal inhibitory concentration (MIC) found for this fungus by Adrian et al.  
470 (1997). Taking into account that the release of an active agent into the medium involves  
several factors, such as solvent and migrant polarities and solubility (Sánchez-González

472 et al. 2011b), the low chemical affinity and solubility of resveratrol with the aqueous  
solvent could explain the observed effect.

474

#### 4. Conclusions

476 Resveratrol was efficiently incorporated into chitosan and methylcellulose films. These  
composite films showed some changes in their microstructural and physicochemical  
478 properties, especially when the highest concentration of resveratrol was used: their  
water vapour and oxygen barrier properties were hardly affected by the induced  
480 structural changes, which implied changes in the semi-crystalline arrangement of CH  
and MC and the appearance of resveratrol crystals in the more concentrated MC films.

482 Nevertheless, films became less stretchable and resistant to fracture, more opaque and  
less glossy due to structural changes provoked by resveratrol in the matrix, although  
484 from a practical point of view, these changes did not negatively affect to the handle,  
manipulation or appearance of the films.

486 Composite films also exhibited antioxidant activity, which was proportional to the  
resveratrol concentration used and no notable losses of this activity during film  
488 formation and conditioning were observed. None of the films showed antimicrobial  
activity against *P. italicum* and *B. cinerea*.

490 The obtained results points out that resveratrol based films are suitable for coating  
purposes. The coating of food products with these films could minimize or prevent  
492 oxidation processes, maintaining nutritional quality, and prolonging the food shelf life.  
Thus, future studies will focus on the applications of these films to food products which  
494 are sensitive to oxidative processes.

#### 496 5. Acknowledgements

The authors acknowledge the financial support from the Spanish Ministerio de Ciencia  
498 e Innovación throughout the project AGL2010-20694.

## 500 6. References

Adrian, M., Jeandet, P., Veneau, J., Weston, L.A., & Bessis, R. (1997). Biological  
502 activity of resveratrol, a stilbenic compound from grapevines, against *Botrytis*  
*cinerea*, the causal agent for gray mold. *Journal of Chemical Ecology*, 23, 1689-  
504 1702.

ASME. (1995). Surface texture: Surface roughness, waviness and lay. Standard  
506 Designation: ASME B46.1. An American National Standard. New York, USA.

ASTM. (2005). Standard test method for oxygen gas transmission rate through plastic  
508 film and sheeting using a Coulometric sensor. Standard Designation: D3985-05. In:  
Annual Book of American Society for Testing Materials, West Conshohocken, PA,  
510 USA.

ASTM. (1999). Standard test method for specular gloss. Standard Designation: D523-  
512 89. In: Annual Book of American Society for Testing Materials, West  
Conshohocken, PA, USA.

ASTM. (1995). Standard test methods for water vapor transmission of materials.  
Standard Designations: E96-95. In: Annual Book of American Society for Testing  
516 Materials, West Conshohocken, PA, USA.

Brand-Williams, W., Cuvelier, M.E., & Berset, C. (1995). Use of a free radical method  
518 to evaluate antioxidant activity. *LWT-Food Science and Technology*, 28, 25-30.

Caruso, F., Tanski, J., Villegas-Estrada, A., & Rossi, M. (2004). Structural basis for  
520 antioxidant activity of trans-resveratrol: Ab initio calculations and crystal and  
molecular structure. *Journal of Agricultural and Food Chemistry*, 52, 7279-7285.



- 522 Donhowe, I.G., & Fennema, O.R. (1993a). The effects of plasticizers on crystallinity,  
permeability, and mechanical properties of methylcellulose films. *Journal of Food*  
524 *Processing and Preservation*, 17, 247-257.
- Donhowe, I.G., & Fennema, O.R. (1993b). The effects of solution composition and  
526 drying temperature on crystallinity, permeability and mechanical properties of  
methylcellulose films. *Journal of Food Processing and Preservation*, 17, 231-246.
- 528 Filip, V., Plockova, M., Smidrkal, J., Spickova, Z., Melzoch, K., & Schmidt, S. (2003).  
Resveratrol and its antioxidant and antimicrobial effectiveness. *Food Chemistry*, 83,  
530 585-593.
- Gennadios, A., Weller, C.L., & Gooding, C.H. (1994). Measurement errors in water  
532 vapor permeability of highly permeable, hydrophilic edible films. *Journal of Food*  
*Engineering*, 21, 395-409.
- 534 Gülçin, I. (2010). Antioxidant properties of resveratrol: A structure-activity insight.  
*Innovative Food Science and Emerging Technologies*, 11, 210-218.
- 536 Hoos, G., & Blaich, R. (1990). Influence of resveratrol on germination of conidia and  
mycelium growth of *Botrytis cinerea* and *Phomopsis viticola*. *Journal of*  
538 *Phytopathology*, 129, 102-110.
- Hutchings, J.B. (1999). *Food Color and Appearance*, 2<sup>nd</sup> ed. Ed. Aspen Publishers, Inc.,  
540 Gaithersburg, Maryland, USA.
- Kristo, E., Koutsoumanis, K.P., & Biliaderis, C.G. (2008). Thermal, mechanical and  
542 water vapor barrier properties of sodium caseinate films containing antimicrobials  
and their inhibitory action on *Listeria monocytogenes*. *Food Hydrocolloids*, 22, 373-  
544 386.
- Krochta, J.M., & Mulder-Johnston, C. (1997). Edible and biodegradable polymer films:  
546 challenges and opportunities. *Food Technology*, 51, 61-74.

- Li, Q., Dunn, E.T., Grandmaison, E.W., & Goosen, M.F.A. (1992). Applications and  
548 properties of chitosan. In: Goosen, M.F.A (Ed.), Applications of chitin and chitosan.  
Technomic Publishing Co. Inc., pp. 3-29.
- 550 López-Nicolás, J.M., & García-Carmona, F. (2010). Effect of hydroxypropyl- $\beta$ -  
cyclodextrin on the aggregation of (E)-resveratrol in different protonation states of  
552 the guest molecule. *Food Chemistry*, 118, 648-655.
- López-Nicolás, J.M., & García-Carmona, F. (2008). Rapid, simple and sensitive  
554 determination of the apparent formation constants of *trans*-resveratrol complexes  
with natural cyclodextrins in aqueous medium using HPLC. *Food Chemistry*, 109,  
556 868-875.
- Matthäus, B. (2002). Antioxidant activity of extracts obtained from residues of different  
558 oilseeds. *Journal of Agricultural and Food Chemistry*, 50, 3444-3452.
- Miller, K.S., & Krochta, J.M. (1997). Oxygen and aroma barrier properties of edible  
560 films: A review. *Trends in Food Science and Technology*, 81, 228-237.
- Murcia, M.A., & Martínez-Tomé, M. (2001). Antioxidant activity of resveratrol  
562 compared with common food additives. *Journal of Food Protection*, 64, 379-384.
- Pastor, C., Sánchez-González, L., Cháfer, M., Chiralt, A., & González-Martínez, C.  
564 (2010). Physical and antifungal properties of hydroxypropylmethylcellulose based  
films containing propolis as affected by moisture content. *Carbohydrate Polymers*,  
566 82, 1174-1183.
- Sánchez-González, L., Chiralt, A., González-Martínez, C., & Cháfer, M. (2011a). Effect  
568 of essential oils on properties of film forming emulsions and films based on  
hydroxypropylmethylcellulose and chitosan. *Journal of Food Engineering*, 105,  
570 246-253.

- Sánchez-González, L., Cháfer, M., González-Martínez, C., Chiralt, A., & Desobry, S.  
572 (2011b). Study of the release of limonene present in chitosan films enriched with  
bergamot oil in food simulants. *Journal of Food Engineering*, 105, 138-143.
- 574 Sánchez-González, L., González-Martínez, C., Chiralt, A., & Cháfer, M. (2010).  
Physical and antimicrobial properties of chitosan-tea tree essential oil composite  
576 films. *Journal of Food Engineering*, 98, 443-452.
- Sánchez-Moreno, C., Larrauri, J.A., & Saura-Calixto, F. (1998). A procedure to  
578 measure the antiradical efficiency of polyphenols. *Journal of the Science of Food  
and Agriculture*, 76, 270-276.
- 580 Soto-Valdez, H., Auras, R., & Peralta, E. (2011). Fabrication of Poly(lactic acid) films  
with resveratrol and the diffusion of resveratrol into ethanol. *Journal of Applied  
582 Polymer Science*, 121, 970-978.
- Vargas, M., Perdonés, A., Chiralt, A., Cháfer, M., & González-Martínez, C. (2011a).  
584 Effect of homogenization conditions on physicochemical properties of chitosan-  
based film-forming dispersions and films. *Food Hydrocolloids*, 25, 1158-1164.
- 586 Vargas, M., Albors, A., Chiralt, A., & González-Martínez, C. (2011b). Water  
interactions and microstructure of chitosan-methylcellulose composite films as  
588 affected by ionic concentration. *LWT-Food Science and Technology*, 44, 2290-2295.
- Villaño, D., Fernández-Pachón, M.S., Moyá, M.L., Troncoso, A.M., & García-Parrilla,  
590 M.C. (2007). Radical scavenging ability of polyphenolic compounds towards DPPH  
free radical. *Talanta*, 71, 230-235.
- 592 Wan, Y., Wu, H., & Wen, D. (2006). Biodegradable polylactide/chitosan films blend  
membranes. *Biomacromolecules*, 7, 1362-1372.

- 594 Zhang, C., Ding, Y., Ping, Q., & Yu, L.L. (2006). Novel chitosan derived nanomaterials  
and their micelle-forming properties. *Journal of Agricultural and Food Chemistry*,  
596 54, 8409-8416.

ACCEPTED MANUSCRIPT

**Highlights**

- Resveratrol was efficiently incorporated into both chitosan and methylcellulose films.
- Composite films exhibited antioxidant properties but no antifungal activity against *P.italicum* and *B. cinerea*.
- Barrier properties, films' mechanical resistance, gloss and transparency decreased in composite films, especially when using the highest resveratrol concentration.
- Resveratrol incorporation induced changes in the semi-crystalline arrangement of CH and MC, and the appearance of resveratrol crystals in the more concentrated MC films.

**Table 1.-** Thickness, moisture content, water vapour permeability (WVP) and oxygen permeability (OP) of films equilibrated at 25°C and 75% RH. Mean values and standard deviation.

| <b>Film</b> | <b>Thickness<br/>(<math>\mu\text{m}</math>)</b> | <b>Moisture content<br/>(g H<sub>2</sub>O/ g ss)</b> | <b>WVP<br/>(g/Pa s m)x10<sup>10</sup></b> | <b>OP<br/>(cm<sup>3</sup><math>\mu\text{m}</math>/m<sup>2</sup> d kPa)</b> |
|-------------|---|--|---|--|
| MC          | 51 (4) <sup>a</sup>                             | 7.0 (0.7) <sup>b</sup>                               | 8.7 (0.9) <sup>b</sup>                    | 127 (20) <sup>a</sup>  |
| MC+R10      | 51 (3) <sup>a</sup>                             | 6.73(0.13) <sup>ab</sup>                             | 7.7 (0.7) <sup>c</sup>                    | 125 (33) <sup>a</sup>  |
| MC+R100     | 58 (9) <sup>b</sup>                             | 5.9 (0.3) <sup>a</sup>                               | 6.0 (0.6) <sup>d</sup>                    | 121 (25) <sup>a</sup>  |
| CH          | 58 (6) <sup>b</sup>                             | 14.9 (0.7) <sup>c</sup>                              | 12 (1) <sup>a</sup>                       | 14.4 (0.5) <sup>b</sup>  |
| CH+R10      | 61 (7) <sup>b</sup>                             | 14.53 (0.13) <sup>c</sup>                            | 12 (2) <sup>a</sup>                       | 16 (1) <sup>b</sup>  |
| CH+R100     | 74 (5) <sup>c</sup>                             | 19.0 (0.5) <sup>d</sup>                              | 11.9 (0.5) <sup>a</sup>                   | 11.2 (0.4) <sup>b</sup>  |

<sup>a,b,c,d</sup> Different superscripts within a column indicate significant differences

among films (p<0.05)

**Table 2.-** Elastic modulus (EM) and tensile strength (TS), and percentage of elongation (E) at break of films equilibrated at 25°C and 75% RH. Mean values and standard deviation.

| <b>Film</b> | <b>TS<br/>(MPa)</b>  | <b>EM<br/>(MPa)</b>     | <b>E<br/>(%)</b>       |
|-------------|----------------------|-------------------------|------------------------|
| MC          | 66 (6) <sup>b</sup>  | 1604 (92) <sup>a</sup>  | 15 (2) <sup>c</sup>    |
| MC+R10      | 65 (7) <sup>b</sup>  | 1871 (132) <sup>b</sup> | 10 (3) <sup>b</sup>    |
| MC+R100     | 49 (5) <sup>a</sup>  | 1903 (55) <sup>b</sup>  | 4 (1) <sup>a</sup>     |
| CH          | 94 (15) <sup>d</sup> | 2739 (93) <sup>d</sup>  | 14 (7) <sup>c</sup>    |
| CH+R10      | 78 (2) <sup>c</sup>  | 2585 (151) <sup>c</sup> | 6 (2) <sup>a</sup>     |
| CH+R100     | 43 (5) <sup>a</sup>  | 1550 (195) <sup>a</sup> | 5.1 (0.4) <sup>a</sup> |

<sup>a,b,c,d</sup> Different superscripts within a column indicate

significant differences among films ( $p < 0.05$ ).

**Table 3.-** Lightness ( $L^*$ ), chrome ( $C^*_{ab}$ ), hue ( $h^*_{ab}$ ), whiteness index (WI) and gloss at  $60^\circ$  of films equilibrated at  $25^\circ\text{C}$  and 75% RH. Mean values and standard deviation.

| Film    | $L^*$                   | $C^*_{ab}$              | $h^*_{ab}$              | WI                  | Gloss $60^\circ$ (GU) |
|---------|-------------------------|-------------------------|-------------------------|---------------------|-----------------------|
| MC      | 83.8 (0.8) <sup>d</sup> | 11.3 (0.8) <sup>a</sup> | 85.7 (0.8) <sup>c</sup> | 80 (1) <sup>d</sup> | 52 (13) <sup>c</sup>  |
| MC+R10  | 64 (1) <sup>a</sup>     | 20 (1) <sup>d</sup>     | 77 (1) <sup>b</sup>     | 59 (1) <sup>a</sup> | 33 (13) <sup>b</sup>  |
| MC+R100 | 63 (1) <sup>a</sup>     | 19.7 (0.6) <sup>d</sup> | 72 (1) <sup>a</sup>     | 58 (1) <sup>a</sup> | 18 (6) <sup>a</sup>   |
| CH      | 80.7 (0.4) <sup>c</sup> | 15.5 (0.6) <sup>b</sup> | 89.3 (0.6) <sup>e</sup> | 75 (1) <sup>c</sup> | 47 (13) <sup>c</sup>  |
| CH+R10  | 79 (1) <sup>b</sup>     | 18 (2) <sup>c</sup>     | 88 (1) <sup>d</sup>     | 72 (2) <sup>b</sup> | 36 (14) <sup>b</sup>  |
| CH+R100 | 81 (2) <sup>c</sup>     | 17 (3) <sup>c</sup>     | 90 (2) <sup>e</sup>     | 75 (3) <sup>c</sup> | 20 (6) <sup>a</sup>   |

<sup>a,b,c,d,e</sup> Different superscripts within a column indicate significant

differences among films ( $p < 0.05$ ).



**Table 4.-** Efficient concentration ( $EC_{50}$ ) (amount of antioxidant needed to reduce the initial DPPH $\cdot$  concentration to 50%, once the steady-state of the reaction was reached) of pure resveratrol (R) and the different films.

| <b>Film</b> | <b><math>EC_{50}</math><br/>(moles R/mole DPPH<math>\cdot</math>)</b> | <b><math>EC_{50}</math><br/>(kg film/mole DPPH<math>\cdot</math>)</b> |
|-------------|---|---|
| R           | 0.70 (0.07) <sup>b</sup>  | -   |
| MC+R10      | 0.95 (0.12) <sup>a</sup>  | 24 (3)  |
| MC+R100     | 0.87 (0.05) <sup>a</sup>  | 2.16 (0.13)   |
| CH+R10      | 0.71 (0.04) <sup>b</sup>  | 19 (1)  |
| CH+R100     | 0.73 (0.07) <sup>b</sup>  | 2.0 (0.2)   |

<sup>a,b</sup> Different superscripts within a column indicate significant differences among films ( $p < 0.05$ ).

**Figure captions**

**Figure 1.-** SEM micrographs of the cross-sections of the dried films equilibrated with  $P_2O_5$  at 25°C.

**Figure 2.-** AFM micrographs of the surface of the dried films equilibrated with  $P_2O_5$  at 25°C. Mean values and standard deviation of  $R_q$  (nm) and  $R_a$  (nm) roughness parameters.

**Figure 3.-** Phase images of the dried films samples equilibrated with  $P_2O_5$  at 25°C.

**Figure 4.-** Typical curves of tensile strength *versus* Hencky deformation of films equilibrated at 25°C and 75% RH.

**Figure 5.-** Spectral distribution of internal transmittance ( $T_i$ ) of films equilibrated at 25°C and 75% RH.

**Figure 6.-** Decrease of  $DPPH\cdot$  as a function of the number of moles of resveratrol per mole of  $DPPH\cdot$ .

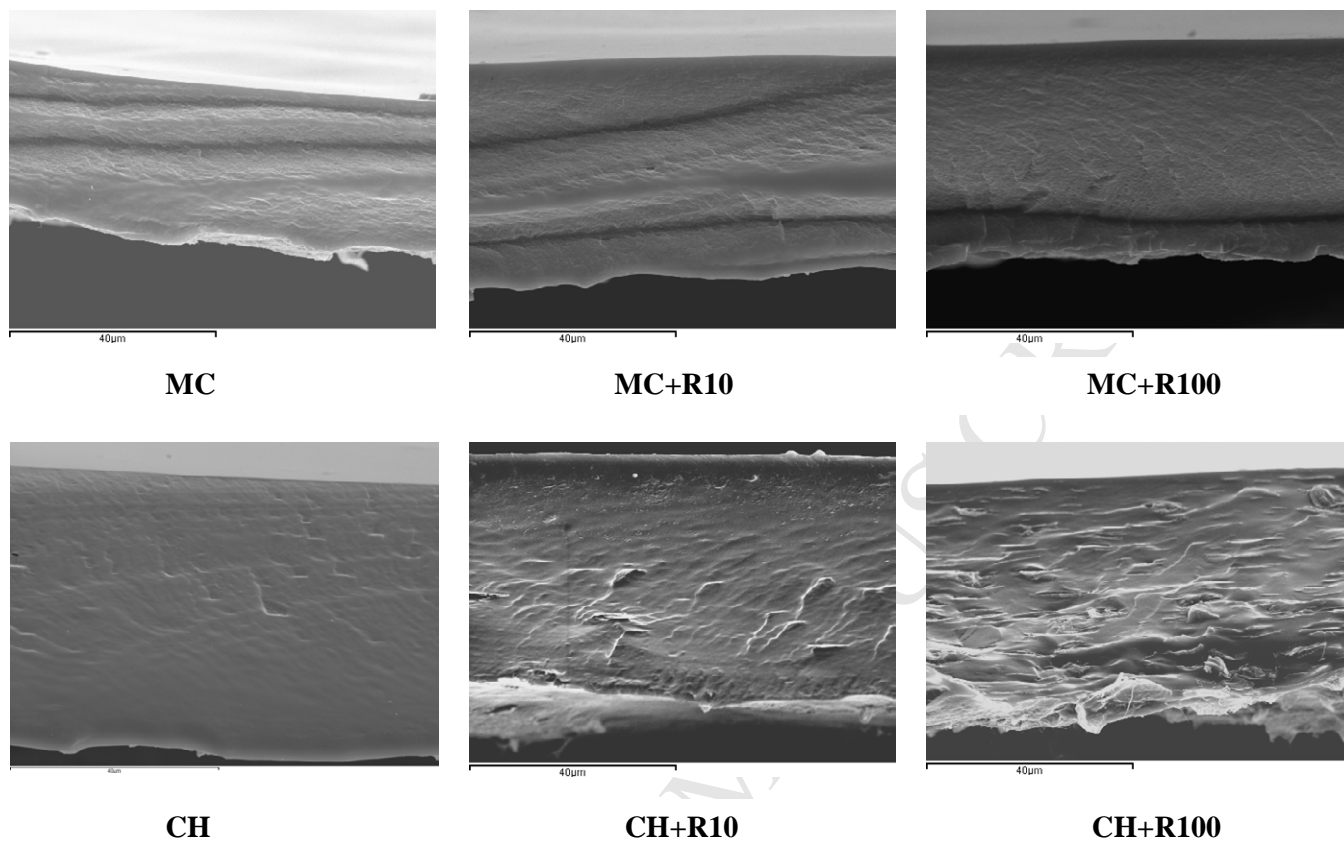


**Figure 1**

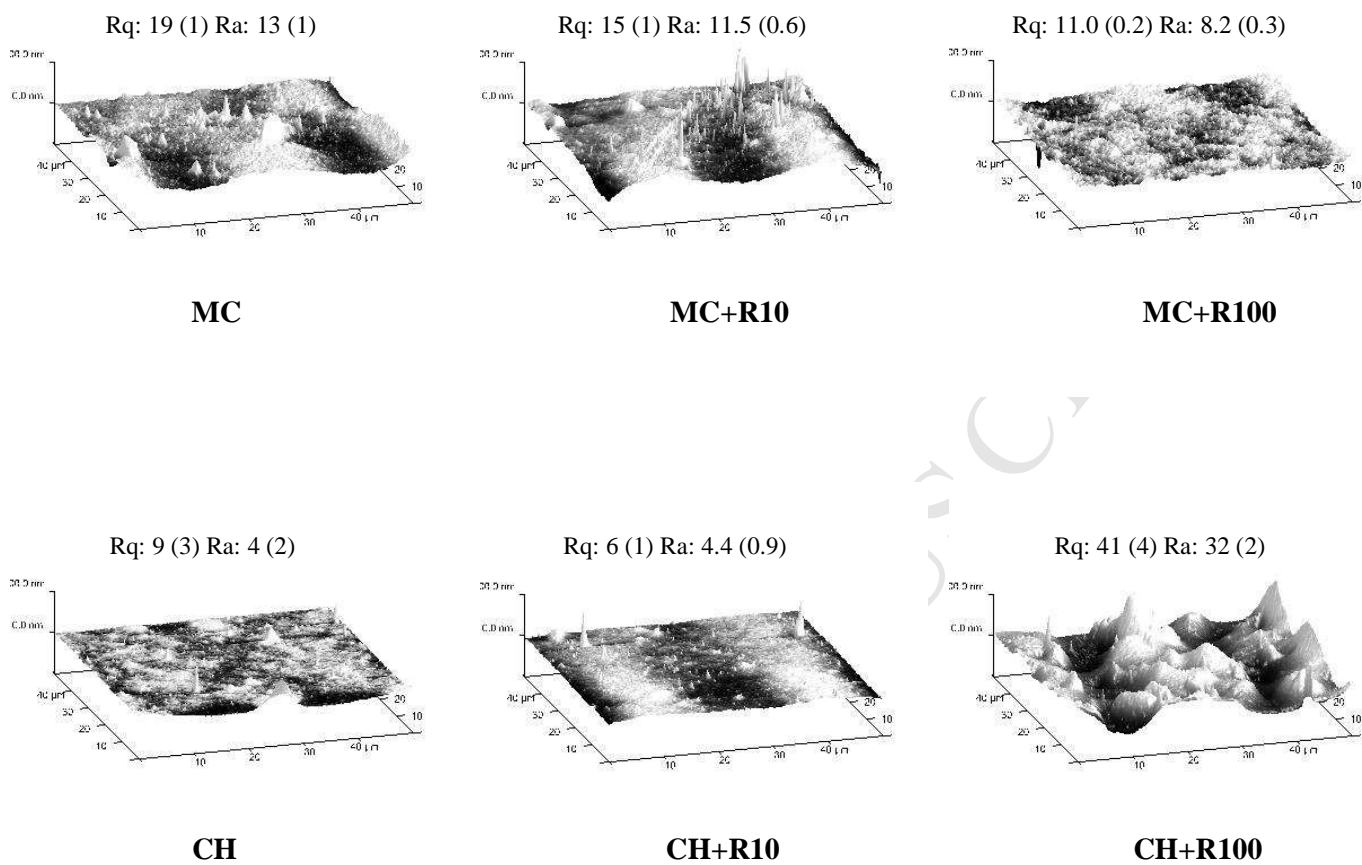


Figure 2

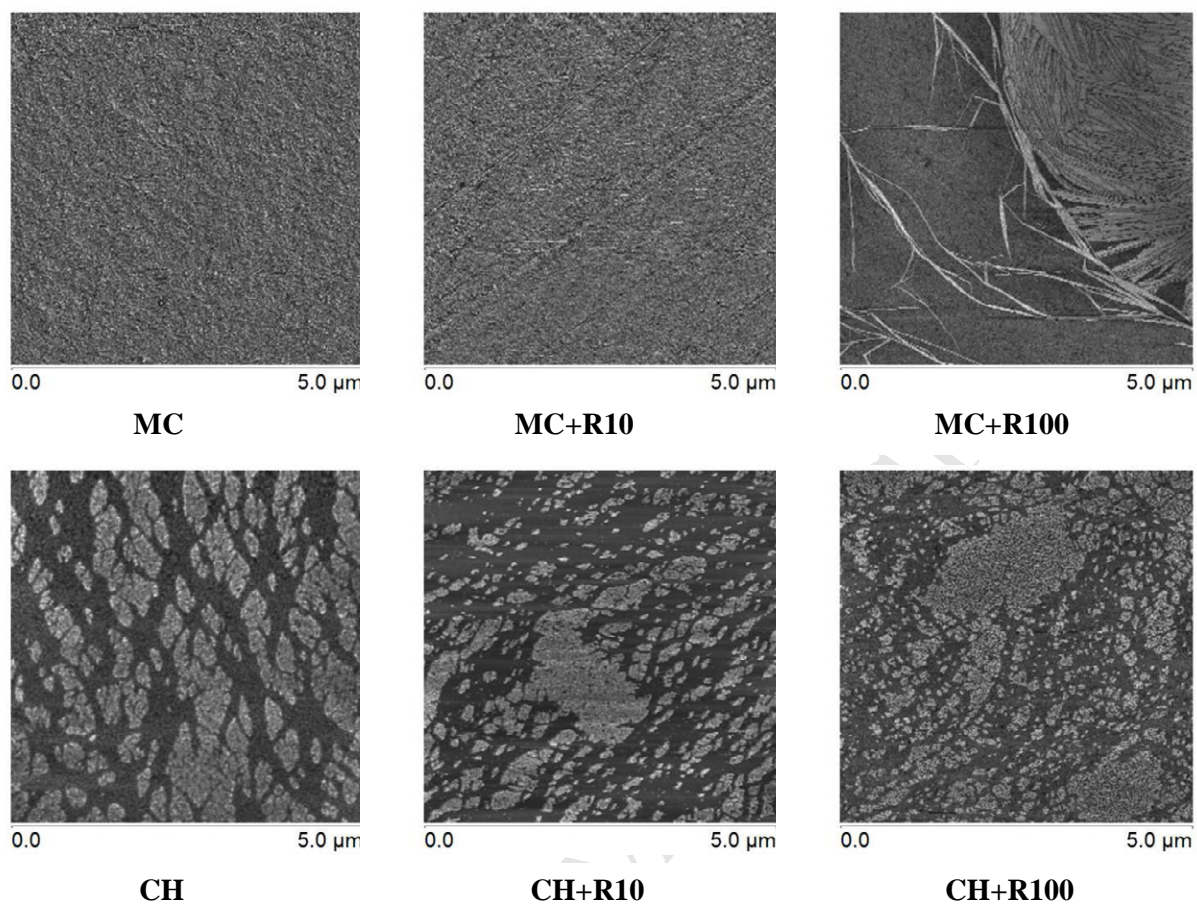
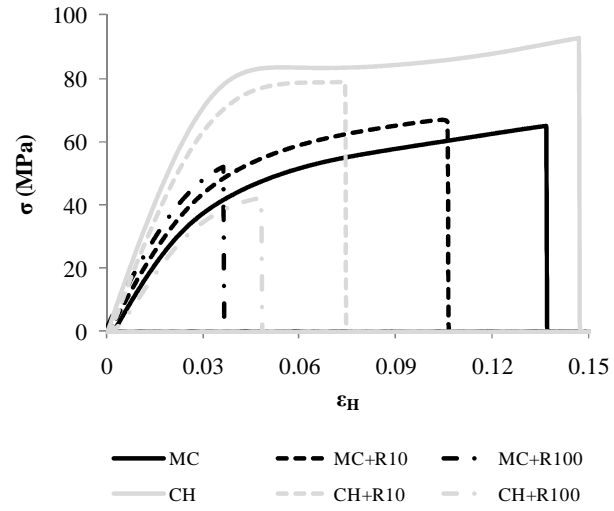


Figure 3

**Figure 4**

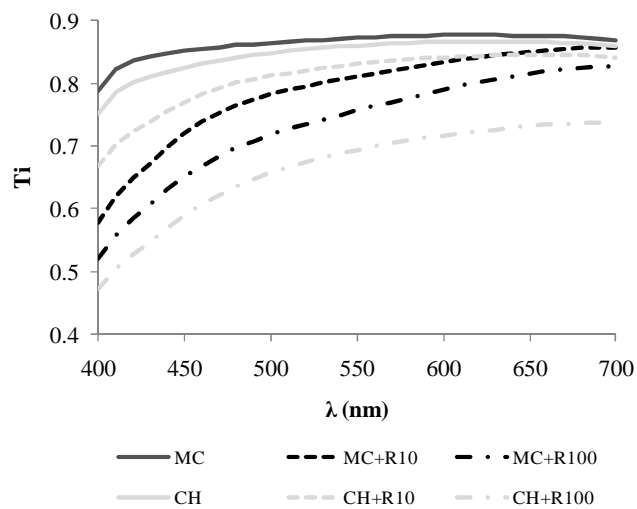


Figure 5

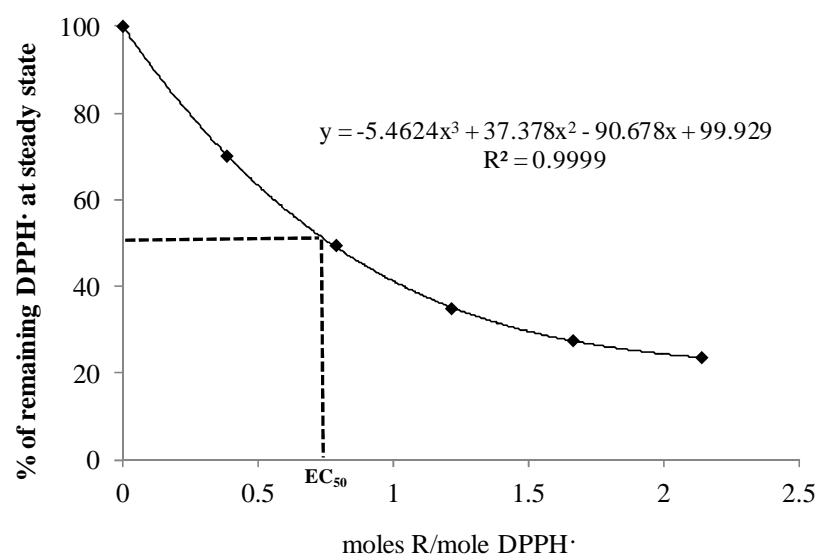


Figure 6